Published in final edited form as:
Clin Exp Allergy. 2005 July ; 35(7): 894–906. doi:10.1111/j.1365-2222.2005.02271.x.

Airway generation-specific differences in the spatial distribution of immune cells and cytokines in allergen-challenged rhesus monkeys

L. A. Miller[*], **S. D. Hurstw**[†,1], **R. L. Coffmanw**[†,2], **N. K. Tyler**[*], **M. Y. Stovall**[*], **D. L. Chou**[*], **L. F. Putney**[*], **L. J. Gershwin**[*], **E. S. Schelegle**[*], **C. G. Plopper**[*], and **D. M. Hyde**[*]

[*]Center for Comparative Respiratory Biology and Medicine and the California Regional Primate Research Center, University of California, Davis, CA

[†]DNAX Research Institute, Palo Alto, CA

[1]Department of Immunology, Genentech, One DNA Way, South San Francisco, CA 94080.

[2]Dynavax Technologies, 717 Potter Street, Suite 100, Berkeley, CA 94710.

Summary

Background—Accumulation of immune cell populations and their cytokine products within tracheobronchial airways contributes to the pathogenesis of allergic asthma. It has been postulated that peripheral regions of the lung play a more significant role than proximal airways with regard to inflammatory events and airflow obstruction.

Objective—To determine whether immune cell populations and associated cytokines are uniformly distributed throughout the conducting airway tree in a non-human primate model of allergic asthma.

Methods—We used a stereologic approach with a stratified sampling scheme to measure the volume density of immune cells within the epithelium and interstitium of trachea and 4–5 intrapulmonary airway generations from house dust mite (HDM) (Dermatophagoides farinae)-challenged adult monkeys. In conjunction with immune cell distribution profiles, mRNA levels for 21 cytokines/ chemokines and three chemokine receptors were evaluated at four different airway generations from microdissected lungs.

Results—In HDM-challenged monkeys, the volume of $CD1a^+$ dendritic cells, $CD4^+$ T helper lymphocytes, $CD25^+$ cells, IgE^+ cells, eosinophils, and proliferating cells were significantly increased within airways. All five immune cell types accumulated within airways in unique patterns of distribution, suggesting compartmentalized responses with regard to trafficking. Although cytokine mRNA levels were elevated throughout the conducting airway tree of HDM-challenged animals, the distal airways (terminal and respiratory bronchioles) exhibited the most pronounced up-regulation.

Conclusion—These findings demonstrate that key effector immune cell populations and cytokines associated with asthma differentially accumulate within distinct regions and compartments of tracheobronchial airways from allergen-challenged primates.

Correspondence: Lisa A. Miller, Department of Anatomy, Physiology, and Cell Biology, School of Veterinary Medicine, University of California, Davis, CA 95616, USA. lmiller@ucdavis.edu.

Keywords

CD25; dendritic cell; dermatophagoides farinae; eosinophil; IgE; lung; primate; T lymphocyte

Introduction

Atopic asthma is a chronic inflammatory disease of the lungs, characterized by airflow obstruction and bronchial hyper-reactivity in response to allergen inhalation. Based on findings from human studies and animal models, it is apparent that many different immune cells and cytokines are involved in the pathogenesis of asthma (reviewed in [1]). Evaluation of airway biopsies and lavage fluids has been a useful approach in determining the key cellular components and mediators that are immunomodulated in human asthmatic subjects. This approach has been utilized to demonstrate enhanced accumulation of antigen-presenting dendritic cells, activated T helper (Th) cells, and eosinophils within biopsy specimens obtained from atopic asthmatics [2-8]. IgE antibodies are central to the establishment of allergy; evidence of local (airway) synthesis includes the identification of mature epsilon heavy chain-containing cells in the nasal mucosa of patients with allergic rhinitis and increased allergen-specific IgE within bronchoalveolar lavage after segmental allergen challenge of atopic asthmatics [9, 10]. Cytokines, chemokines, and corresponding receptors associated with recruitment and effector functions of all of the aforementioned immune cell types (i.e. IL-4, monocyte-derived chemokine (MDC), CCR3) have also been reported to be elevated in biopsy and lavage of patients with asthma (reviewed in [11-13]).

Histopathology of lung sections obtained post-mortem from patients with asthma indicates that immune cells accumulate throughout the entire conducting airway tree [14-17]. Disregarding compartments (epithelium or interstitium), comparative analysis of large vs. small airways in asthmatics shows no difference with regard to overall number of lymphocytes and eosinophils [15, 17]. However, Hamid et al. [17] do report a significant increase in activated $EG2^+$ eosinophils within airways less than 2 mm in perimeter, suggesting that the peripheral lung environment plays an important role in eosinophil effector functions. When the subepithelial space is separated into defined regions, comparison of large cartilaginous airways (perimeter >3.0 mm) and small airways (perimeter <3.0 mm) from patients with severe asthma or cystic fibrosis shows differential distribution of inflammatory cells with regard to compartments [14]. Specifically, larger airways of asthmatics are characterized by a higher density of $CD45^+$ leucocytes and eosinophils within an inner ‘ring’ comprised of the space between basement membrane and smooth muscle, as compared with an outer interstitial ring comprised primarily of smooth muscle. In small airways, this relationship is reversed; $CD45^1$ leucocytes and eosinophils predominantly accumulate within the outer interstitial ring of small airways as compared with the inner region. Available data on spatial distribution of cytokine and chemokine expression are limited. It has been reported that small airways contain more cells expressing IL-5 mRNA as compared with large airways; the majority of IL-5 expressing cells are $CD3^+$ T lymphocytes [18]. Although strong histopathological and molecular evidence suggests that immune cell populations and mediators accumulate differentially within large vs. small airways, specific airway generations and compartments (i.e. epithelium vs. interstitium) have not yet been defined in this manner in an animal model.

To address this issue, we have utilized stereological approaches to map the distribution of $CD1a^+$ dendritic cells, $CD4^+$ Th cells, $CD25^+$ activated cells, IgE^+ cells, eosinophils, and proliferating cells within either epithelial or interstitial compartments throughout the length of the conducting airway tree. We have previously reported that sensitization and challenge of adult rhesus macaque monkeys to the relevant human allergen, house dust mite (HDM),

result in the development of immunological, physiological, and structural parameters consistent with human allergic asthma [19]. In this current study, we have utilized histological specimens from the aforementioned study to compare the distribution of immune cells throughout the conducting airway tree. In conjunction with histopathological analysis, we have also assessed airway generation-specific tissue samples from this study to determine the mRNA levels for a panel of 21 cytokines/chemokines and three chemokine receptors. Our findings indicate that there are regional differences in the distribution of key effector cell types in asthma throughout the conducting airways, as well as by compartment (epithelial vs. interstitial). In addition, by molecular analysis of immune mediators throughout the conducting airways of HDM-challenged monkeys, we also show that mRNA expression of key cytokines and chemokines in asthma is dramatically elevated within peripheral airways.

Methods

Animal and experimental protocol

Rhesus macaque *(Macaca mulatta)* monkeys used for this study were previously characterized as a non-human primate model of allergic asthma [19]. Briefly, three adult female monkeys were sensitized by SQ injection of 12.5 μg HDM in 10 μg aluminium hydroxide with 10^{11} killed *Bordetella pertussis*-injected IM. On days 30 and 74 following initial sensitization, monkeys received booster injections of HDM. On days 14, 15, 16, and 46 following initial sensitization, monkeys received 94 mg of HDM instilled intranasally. Subsequently, monkeys were housed in filtered air and exposed to aerosolized HDM (437 ± 69 $\mu g/m^3$ protein) for 2–3 h, three times per week, for approximately 3 months. Control monkeys were rhesus macaques of comparable age that were obtained from the colony and maintained in filtered air; controls had negative skin tests for HDM. Monkeys were necropsied at 24 h post-allergen aerosol exposure as described in [19]. All animals received an injection of 5-bromo-2′deoxyuridine (BrdU; 30 mg/kg) at 1 h prior to necropsy; this concentration has been reported to be sufficient for cellular labelling with minimal toxicity in rhesus monkeys [20]. All aspects of animal work were performed in accordance with institutional guidelines for the California National Primate Research Center.

Histopathology/immunohistochemistry

Following necropsy, cross-sections of trachea and the entire right middle lobe from each animal were fixed by inflation with glutaraldehyde/paraformaldehyde (1%/1%), and sliced perpendicular to the long axis of the intrapulmonary airway. To allow for progressive proximal to distal sampling of intrapulmonary airways, each right middle lobe slice was numbered in sequence prior to embedding in Araldite. Two micrometre plastic sections from alternately numbered Araldite blocks were sampled; airway generations in blocks derived from the right middle lobe were defined as proximal (P1 and P2) and midlevel (M1 and M2). For the quantitation of eosinophils, haematoxylin and eosin (H&E)-stained thin plastic sections were used for optimal resolution of cellular structure.

For all other immune cell types, quantitation was performed on cryosections prepared from the trachea and left caudal lobe of each animal. The left caudal lobe was inflated with a 1 : 1 mixture of OCT freezing compound (Sakura Finetek, Torrance, CA, USA) and phosphate-buffered saline (PBS) and sliced perpendicular to the long axis of the intrapulmonary airway. As with the right middle lobe, each left caudal lobe slice was numbered in sequence prior to freezing in OCT moulds. Tissue blocks were cut in to approximately 7–8 mm thicknesses; the entire lung lobe consisted of 13–14 blocks. Five micron frozen sections from alternately numbered OCT blocks were used for immunofluorescence and immunohistochemical staining. Airway generations in blocks derived from the left caudal

lobe were defined as proximal (P1 and P2), midlevel (M1 and M2), and respiratory bronchiole (RB).

For immunofluorescence staining, 5 μm cryosections of the left caudal lobe and trachea were fixed in ice-cold acetone for 10 min and allowed to dry. To block non-specific binding of antibodies, cryosections were incubated for 10 min with purified goat IgG (10 μg/mL; Sigma, St Louis, MO, USA) or donkey IgG (10 μg/mL; Jackson ImmunoResearch Laboratories, Westgrove, PA, USA) at RT. Cryosections were then stained with (1) fluorescein isothiocynate-conjugated mouse anti-human CD1a monoclonal antibody (1 μg/mL; BD Biosciences Pharmingen, San Diego, CA, USA) or (2) mouse anti-human CD4 monoclonal antibody (tissue culture super-natent from clone OKT4; ATCC, Manassas, VA, USA), and fluorescein isothiocynate-conjugated mouse anti-human CD25 monoclonal antibody (1 μg/mL; Becton Dickinson Immunocytometry, San Jose, CA, USA), or (3) mouse anti-human CD4 monoclonal antibody and biotinylated mouse anti-rhesus CD3 monoclonal antibody (1 μg/mL; Biosource, Camarillo, CA, USA), or (4) goat anti-human IgE polyclonal antibody (1 μg/mL; Bethyl Labs, Montgomery, TX, USA). ALEXA 568-conjugated goat anti-mouse IgG, ALEXA 488-conjugated donkey anti-goat IgG, and ALEXA 488-conjugated streptavidin from Molecular Probes (Eugene, OR, USA) were used as secondary detection reagents for anti-CD4, anti-IgE, and anti-CD3 antibodies (1 : 1000 dilution). Cellular incorporation of BrdU was detected by staining acetone-fixed cryosections with a mouse anti-BrdU monoclonal antibody purchased from DAKO (Carpinteria, CA, USA), followed by a biotinylated goat anti-mouse IgG (Vector Laboratories, Burlingame, CA, USA), an avidin-bound peroxidase complex (ABC Vectastain peroxidase mouse IgG kit, Vector Laboratories) and 3,3′-diaminobenzidine (Sigma, St Louis, MO, USA). Appropriate isotype control immunoglobulins (Sigma) were tested with all antibodies used in quantitation of immune cell types.

Morphometry

Eosinophils and $BrdU^+$ cells within stained lung sections were quantitated with an Olympus BH-2 microscope and the CAST version 2.00.04 software (Olympus, Ballerup, Denmark) at × 400. A minimum of 10 fields per block were selected using stratified sampling with a random start. Using the eosinophil as an example, points of a 16-point grid that fell on eosinophils were counted (P_{eos}) and those points that fell on either epithelium or interstitium were counted as the reference volume of the epithelium (P_{epi}) or interstitium (P_{int}). The volume density of eosinophils per volume of epithelium or interstitium was calculated as

$$V_{\nu_{\mathrm{eos},(\mathrm{epi\ \ or\ \ int})}} = \frac{\sum P_{\mathrm{eos}}}{\sum P_{\mathrm{epi}} \text{ or } \sum P_{\mathrm{int}}}$$

The surface of epithelial basal lamina per unit volume of epithelium $S_{\nu_{\mathrm{bl;epi}}}$ or interstitium ($S_{\nu_{\mathrm{bl;int}}}$) was calculated on cross-sections of airways at × 100 using an Olympus BH-2 microscope with the CAST version 2.00.04 software (Olympus) as

$$S_{\nu_{\mathrm{bl},(\mathrm{epi\ \ or\ \ int})}} = \frac{\pi \sum I_{\mathrm{bl}}}{2\,(l/p)\,(P_{\mathrm{epi}} \text{ or } P_{\mathrm{int}})}$$

where l/p is the length per test point on four lines oriented either horizontally or vertically in a counting frame, I_{bl} is the number of line intersections of the epithelial basal lamina, and P_{epi} or P_{int} the number of points that hit epithelium or interstitium, respectively. The volume of eosinophils within the epithelial or interstitial compartment per surface area of basement membrane (mm^3/mm^2) was then calculated as

$$V_{s_{\mathrm{eos,bl}}} = \frac{V_{\nu_{\mathrm{eos,(epi\ or\ int)}}}}{S_{\nu_{\mathrm{bl,(epi\ or\ int)}}}}$$

Five micron cryosections of immunostained $CD1a^+$ dendritic cells, $CD4^+$ Th lymphocytes, $CD25^+$ cells, and IgE^+ cells were imaged using the appropriate excitation and emission filters for the cellular-labelled fluorochromes (listed above) on an Olympus Provis Microscope at × 600. Images were captured using a Zeiss camera at a resolution of 150 pixels/in in a 1300 × 1130 pixel image for each of 10 fields for a selected airway, using stratified sampling with a random start within each block. The images were imported into the Stereology Toolbox® (version 1.1, Morphometrix, Davis, CA, USA) for estimation of the volume density of each of the immunostained cells in airway epithelium or interstitium using a 125-point grid. The volume density of each cell type in the epithelium or interstitium and their normalization to the basal laminar surface was performed as described above.

Quantitation of cytokine mRNA by real-time polymerase chain reaction

Immediately following necropsy, specific airway generations were microdissected from the unfixed right caudal lobe of each monkey as previously described in [21]. Each airway sample was snap-frozen in liquid nitrogen, homogenized, and extracted for RNA using TRIzol reagent (Invitrogen, Carlsbad, CA, USA) according to the manufacturer's instructions. cDNA synthesis and real-time PCR analysis were performed as previously described [22]. Briefly, primers were designed using Primer Express software (Applied Biosystems, Foster City, CA, USA), using sequences obtained through the National Center for Biotechnology Information website (http://www.ncbi.nlm.nih.gov/). Using SYBR green buffer (Applied Biosystems), real-time PCR analysis was performed on an ABI PRISM 5700 Sequence Detection System, using default settings for amplification. PCR amplification of the housekeeping gene ubiquitin was performed for each sample to control for sample loading; sample values were normalized with ubiquitin values according to the manufacturer's instructions. There were no significant differences in ubiquitin values for all airway generations sampled (data not shown).

In situ *hybridization*

An IL-4 RNA probe was generated by RT-PCR amplification of a 252 base pair fragment from rhesus monkey lung cDNA, using the primers 5′AACTGCCATATCGCCTTA CG and 5′GTTTCAGGAATCGGATCAGC. Primers for monkey IL-4 were designed using Genbank sequence data for rhesus monkey IL-4 cDNA. The IL-4 PCR product was cloned into a pGEM T-Easy vector (Promega Corporation; Madison, WI, USA), allowing for generation of sense and anti-sense RNA transcripts by SP6 and T7 RNA polymerases. The identity and orientation PCR inserts were verified by sequencing (data not shown). Sense and anti-sense RNA probes were biotinylated using the BrightStar Psoralen-Biotin kit (Ambion; Austin, TX, USA) and assessed via dot blots using avidin conjugated to alkaline phosphatase as a detection medium.

For *in situ* hybridization, frozen sections of the left caudal lobe were dried at room temperature, and then fixed with a 4% paraformaldehyde phosphate buffer for 18 h. After a 5 min proteinase K treatment (50 μg/mL), each airway section was probed with 5 μg of IL-4 sense or anti-sense RNA probe. Sections were allowed to hybridize overnight in a humid chamber at 55 °C. Hybridized sections were then treated with RNAase, washed, and incubated with streptavidin–alkaline phosphatase. NBT/BCIP was used as a substrate for alkaline phosphatase, and colour detection using light microscopy was possible 1.5 h after the substrate was added.

Statistics

Unless indicated, all data are reported as mean ± SE. Groups were compared using a two-way analysis of variance (Stat-view, SAS institute, Cary, NC, USA).

Results

Distribution of immune cells within allergen-challenged airways

We determined whether immune cells associated with the allergic asthma phenotype preferentially accumulate within different tracheobronchial airway generations by assessing cryosections with a stratified sampling approach that allowed for sequential analysis of airway mucosa from the trachea through proximal and distal regions of the left caudal lobe. To identify antigen-presenting cells within airway mucosa of HDM-challenged monkeys, we immunostained lung cryosections with a monoclonal antibody against CD1a, a marker that defines a population of dendritic cells. As shown in Fig. 1a, cells that stain positive for the anti-CD1a antibody within tracheal epithelium have a dendritic appearance. The volume density of $CD1a^+$ dendritic cells within both epithelial and interstitial compartments of HDM-challenged airways was significantly increased; $CD1a^+$ cells were rarely detected in control animals (Figs 1c and d). Within allergen-challenged animals, $CD1a^+$ cells accumulated maximally in the trachea and the most proximal generations of intrapulmonary airways; this was significantly affected within the epithelial compartment ($P<0.0001$).

The distribution of Th cells within tracheobronchial airways was assessed by a combined cell surface staining for CD3 and CD4 in lung cryosections. There was a trend towards elevated volume density of CD3/CD4 fluorescence double-positive cells within the epithelial compartment of airways from HDM-challenged animals (Fig. 2c, $P=0.07$). The volume of $CD4^+$ lymphocytes was significantly elevated within the interstitial compartment of HDM-challenged airways in comparison with controls (Fig. 2d). Both control and HDM monkeys exhibited similar distribution profiles for $CD4^+$ lymphocytes within the epithelial compartment; abundance was highest within the proximal to midlevel intrapulmonary airways. Within the interstitial compartment, there was a significant block-dependent effect of $CD4^+$ lymphocyte accumulation, whereby the volume density of this cell type peaked within the second block of intrapulmonary proximal airway (block P2).

As an index of cellular activation, airway levels were evaluated for expression of CD25, the receptor for IL-2. The volume of $CD25^+$ cells within the epithelium was significantly elevated in HDM-challenged monkeys (Figs 2a and e); very few $CD25^+$ cells were detected in airways of control animals. Within the interstitial compartment, there was a trend toward increased $CD25^+$ cell abundance within HDM-challenged monkeys (Fig. 2f; $P=0.0818$). The volume of interstitial $CD25^+$ cells was highest in the trachea, whereas epithelial $CD25^+$ cells were uniformly distributed for all airway generations examined. Except for the trachea, the volume of $CD25^+$ cells within the epithelial compartment was approximately the same as $CD4^+$ lymphocytes in all airway generations sampled.

The abundance of cells that express IgE or have cell surface-associated IgE was significantly increased in HDM-challenged monkeys. As shown in Fig. 3a, cells that stained positive for an antibody against IgE were of multiple phenotypes; some were defined by a large nucleus and a small amount of cytoplasm, whereas others were large irregularly shaped structures within the interstitium. There was at least a two-fold greater volume of IgE^+ cells within the interstitium as compared with the epithelium in HDM-challenged monkeys (Figs 3b and c). Like $CD1a^+$ and $CD25^+$ cells, the volume of interstitial IgE^+ cells progressively decreased from the most proximal conducting airway (trachea) to the most distal conducting airway

(RB). In contrast, epithelial IgE^+ cells progressively increased in abundance from large to small airways (subsegmental bronchi, terminal bronchioles, and RBs).

Eosinophils were detected within airways by H&E staining of plastic sections and defined as cells containing red granules with bilobed nuclei. The abundance of eosinophils within airways of HDM-challenged monkeys was significantly increased; no eosinophils were detected within the epithelial compartment of control animals (Figs 4a and b). Interstitial eosinophils were most abundant within the trachea. With the exception of the trachea, eosinophil volume within both epithelial and interstitial compartments was similar for all airway generations evaluated in allergen-exposed animals.

Incorporation of BrdU was utilized to detect proliferation of cells within airways following allergen challenge. BrdU labelling was detected within both epithelial and interstitial compartments, and volume significantly increased in HDM monkey airways (Figs 5a and b). Cells labelled with BrdU were primarily found as lymphocyte aggregates within the interstitium; proliferating cells were not $CD3^+$ by immunostaining (data not shown). Although infrequent, some epithelial and interstitial smooth muscle cells were also detected with this stain. Proliferating cells were most abundant within the interstitium of proximal intrapulmonary airways.

Distribution of cytokines, chemokines, and chemokine receptors within allergen-challenged airways

To determine whether cytokine and chemokine expression associated with the allergic asthma phenotype was altered in magnitude throughout large and small airways, we assessed microdissected airways from HDM-challenged monkeys by real-time RT-PCR. As shown in Fig. 6a, tissue samples obtained from trachea, the most proximal portion of the intrapulmonary airway, a midlevel conducting airway (a region containing the last generations of cartilaginous subsegmental bronchi), and RB were assessed for cytokine/chemokine mRNA levels. Because of intraanimal variability, each one of three HDM-challenged animals was compared with a pool of values from five different control animals to determine the relative gene expression levels. Among the 21 cytokines/chemokines evaluated, a number were consistently elevated throughout the sampled airways (although at varying levels), including IL-4, IL-5, MCP-3, and IL-12 p40. In addition, expression of three chemokine receptors, CCR4, CCR5, and CCR7, was elevated in HDM-challenged monkeys relative to controls. In comparing different airway levels, mRNA for a number of cytokines and chemokines were markedly elevated within midlevel airways in two out of three monkeys; the third monkey within the group exhibited this increase within RBs.

To correlate mRNA analysis from tissue samples with histology, *in situ* hybridization was performed on an airway level (block 3) that corresponds to the most prominent site of expression for IL-4. As shown in Fig. 7, multiple cellular phenotypes contain IL-4 mRNA within airways of HDM monkeys. These include clusters of enlarged lymphocytes within the interstitium as well as smaller lymphocytes associated with glands.

Discussion

Because of many similarities with the human immune system and lung architecture, rhesus monkeys serve as an excellent animal model for evaluation of pulmonary mucosal immunity [23-32]. We have previously reported that a defined protocol for HDM exposure of adult rhesus macaque monkeys results in the development of immunological, physiological, and structural parameters consistent with human allergic asthma [19]. Here, we have utilized histological specimens and airway generation-specific tissue samples directly from the aforementioned study to investigate the distribution of immune cells and determine mRNA

levels for a panel of 21 cytokines/ chemokines and three chemokine receptors throughout the conducting airway tree. For each of the five immune cell types evaluated, we have found distinct trafficking patterns throughout the lung that differ by airway generation and subcompartment within the airway wall. The expression profile for cytokine and chemokine mRNA also varied by airway generation; in general, expression of immune mediators was more pronounced in peripheral intrapulmonary conducting airways as compared with proximal airways.

In this study, we have quantitated the abundance of key immune cells for allergic asthma throughout the entire conducting airway tree by sequential analysis starting with the most proximal region (trachea) and ending with the most distal region (RB). In addition, within each airway generation sampled, immune cells were separately evaluated within epithelial and interstitial compartments. For selection of image fields, a stratified sampling approach was used to limit any bias imposed during data collection. Finally, calculation of cellular volume relative to the volume of the epithelial or interstitial compartment sampled (prior to normalization to surface area of basement membrane) is of particular relevance in a disease state that is characterized by inflammation-induced oedema. Concurrent analysis of cytokine/chemokine mRNA levels within defined airway generations from adjacent lung lobes allows for spatial correlation of specific immune cell populations with expression of immune mediators. In the human lung, a similar methodology can be used in tissue samples collected by bronchoscopy. However, this approach is constrained by limited accessibility to distal airways, depth of sampling into the airway wall, and loss of epithelium during the procedure. There are several laboratories that have investigated the distribution of immune cells within the entire wall of both cartilaginous and noncartilaginous human airways; yet, these reports are limited to post-mortem samples or lung resections, which can be problematic with regard to consistent tissue processing [14, 15, 17]. To the best of our knowledge, anatomic investigation of the pulmonary mucosal system throughout the conducting airways has not yet been reported in the literature.

Because the antigen-presenting function of dendritic cells plays a critical role in the priming of immune responses, we evaluated the distribution of this cell type within airway mucosa using CD1a as a marker (Fig. 1). Although there are additional cell surface markers to define immature dendritic cell subpopulations (reviewed in [33]), CD1a has been utilized by several investigators to demonstrate significantly increased numbers of this cell phenotype within biopsy samples of patients with asthma in comparison with control subjects [2- 4, 8]. For the interstitial compartment, our data support the previous findings in human asthmatic subjects. In contrast with Möller and colleagues, we have also found significantly increased abundance of $CD1a^+$ cells within the airway epithelium of HDM monkeys. This apparent discrepancy in findings may be attributed to the frequent loss of epithelium (and therefore limited sampling) because of bronchoscopy [3, 34]. A more recent report confirms the presence of $CD1a^+$ dendritic cells within the human lung, but primarily within the epithelial compartment of both large and small airways; it should be noted that airways were sampled from lung resections and did not include the trachea [35]. In the monkey, $CD1a^+$ dendritic cells preferentially accumulated within the trachea and most proximal intrapulmonary airways; there were few $CD1a^+$ cells within distal intrapulmonary airways regardless of allergen exposure. Further, the volume of $CD1a^+$ cells within the epithelial compartment of proximal airways was roughly equivalent, if not greater than the volume of $CD1a^+$ cells in the interstitial compartment. This pattern of distribution is in contrast with other immune cell types evaluated in this study, where the interstitium appeared to be the primary reservoir for accumulated cells at any particular site. These results suggest that the trachea and proximal intrapulmonary airways are a major site for $CD1a^+$ dendritic cell accumulation.

In human subjects, it has been reported that the overall number of $CD4^+$ lymphocytes within the interstitial compartment of airway mucosa is not significantly different between asthmatics or healthy controls [6]. In this current study, the interstitial volume density of $CD4^+$ lymphocytes within HDM-challenged monkeys was significantly greater as compared with controls, accumulating preferentially within a proximal to midlevel region of the intrapulmonary airways (Fig. 2d). In addition, we observed a trend towards increased abundance of $CD4^+$ lymphocytes within the epithelial compartment of HDM monkey airways as compared with controls (Fig. 2c). This finding has not been reported in human subjects, as the epithelium from bronchoscopy specimens is often problematic to conserve [3, 34]. Th cells play a crucial role in the orchestration of the immune responses that result in the asthma phenotype; yet, bronchoalveolar lavage and biopsy data from human studies do not indicate a substantially increased recruitment of this cell type within the asthmatic lung. *In situ* hybridization and immunohistochemistry cytokine data strongly support a change in effector function by airway T cells, suggesting that it is a shift in phenotype, and not quantity of T lymphocytes that is important [7]. Our data may provide an additional explanation for this apparent discrepancy, by showing that the epithelium may be a significant site for Th cell recruitment and accumulation in the asthma phenotype. Along with Th cell distribution, we also found an increase in the volume of $CD25^+$ cells within both epithelial and interstitial compartments (Figs 2e and f); results for the interstitial compartment are consistent with human studies [5, 6]. A number of different immune cell types can express CD25 upon activation, including Th cells, T cytotoxic cells, B cells, and eosinophils [36-38].

Detection of elevated levels of IgE (total and allergenspecific) within serum is frequently a hallmark parameter of allergy; yet, available data on pulmonary mucosal IgE are limited. Evidence of local IgE synthesis within the airways has been alluded to by molecular analysis of e-chain transcripts, as well as airway lavage [10, 39, 40]. In this study, we have utilized an antibody to detect cells within the airway mucosa that synthesize IgE (mature B cells, plasma cells), as well as cells that have surface IgE (Fig. 3a). In addition to mast cells, a number of cell types within the airway mucosa can express the high-affinity receptor for IgE, Fc eR1, including monocytes, dendritic cells, and epithelium [2, 41]. Within both epithelial and interstitial compartments, the abundance of IgE^+ cells was significantly increased in HDM monkeys (Figs 3c and d). The accumulation of IgE^+ cells within the interstitium was most pronounced within proximal airways, whereas IgE^+ cells within the epithelium were most abundant in distal airways. It was not possible to definitively identify IgE-secreting B lymphocytes from other cell types within the airway mucosa. However, BrdU staining demonstrated a significant increase in abundance of proliferating cells (Fig. 5), the majority of which were detected in germinal centres of lymphoid aggregates from proximal airways (data not shown).

Airway eosinophilia within both lavage and mucosa is a consistent cellular characteristic of asthma [5, 6, 42, 43]. In HDM monkeys, eosinophil volume was significantly elevated within both epithelial and interstitial compartments, but not in a uniform manner throughout the airway tree (Figs 4a and b). Interestingly, we found that eosinophil volume was substantially greater within tracheal interstitium of HDM monkeys (as compared with intrapulmonary airways), whereas the volume within the epithelial compartment remained relatively invariable until the most distal airway generation sampled. We did not evaluate the carina or mainstem bronchi to determine at which point this phenomenon would subside. Regardless, the data suggest that the cellular microenvironment of the trachea preferentially promotes local recruitment of eosinophils from the vasculature. Alternatively, eosinophil trafficking into the airway lumen may be enhanced in the lower airways, thereby depleting and reducing the volume of eosinophils from the interstitium. It is notable that within control animals, no eosinophils were detected within the epithelium of any airway generation

sampled. With the exception of the trachea, a site that is infrequently sampled in the human literature, our findings within the intrapulmonary airways do support the findings of Hamid et al. [17]. Subsequent studies with markers of eosinophil activation may further support a parallel trafficking pattern in the monkey model.

Elevated IL-4 and IL-5 mRNA in bronchial biopsies is a consistent observation in patients with allergic asthma, correlating with serum IgE levels and the severity of asthma [44-47]. As such, it was not unexpected to observe elevated mRNA levels for IL-4 and IL-5 within airways of HDM monkeys (Fig. 6b). Although all generations studied exhibited some degree of increase in IL-4 and IL-5 as compared with controls, mRNA levels for both cytokines were markedly elevated within mid-level (distal bronchus) intrapulmonary airways. For IL-4, our *in situ* hybridization data suggest that multiple cellular phenotypes of lymphoid origin contribute to the airway expression profile for this cytokine (Fig. 7). In parallel with studies from human subjects, IL-13 mRNA expression was elevated within HDM monkeys, primarily within mid-level intrapulmonary airways [48]. mRNA expression for IL-12 p40 was also elevated in two out of three HDM-sensitized and -challenged monkeys. IL-12 has a key regulatory role in Th1 cell differentiation; yet, recent studies demonstrating elevated expression of IL-12 p40 by airway epithelium in asthmatics and in response to viral infection suggest a more generalized role in mucosal defence mechanisms [49].

Of the three different chemokine receptors evaluated in this study, expressions of CCR4 and CCR7 were most pronounced in mid-level intrapulmonary airways and RBs of HDM monkeys. Our finding of increased CCR4 mRNA is consistent with recent reports of increased $CCR4^+$ T cells within airways of patients with asthma at 24 h post-allergen challenge, in conjunction with elevated expression of MDC and thymus- and activated-regulated chemokine by epithelium [12]. CCR7 is primarily expressed on naïve T cells and mature dendritic cells; interaction with its ligand CCL21 is important for trafficking to secondary lymphoid organs [50, 51]. Because it is unlikely that naïve T cells are recruited to the airways, elevated CCR7 can most likely be attributed to increased maturation of dendritic cells. CCR7 expression did not correlate with the localization of $CD1a^+$ dendritic cells in this study. A mature dendritic cell population within the distal intrapulmonary conducting airways may be important for local immune effector responses to allergen exposure. In support of this notion, other investigators have reported the identification of long-lived dendritic cell subsets in the lung that can capture aeroallergen and activate allergen-specific Th cells [52].

One of the goals in this study was to correlate the presence of immune cell phenotypes with expression of specific cytokines/chemokines and receptors. This is based on the assumption that key immune cells in allergic asthma express the most potent combination of cytokines in response to aeroallergen exposure. Identification of critical cellular sources for immunomodulatory cytokines has been problematic for humans, as the immune response to allergens is more complex and heterogeneous as compared with rodent species [53]. We found that mRNA levels for a number of Th2 cytokines, chemokines, and chemokine receptors were markedly elevated within more distal conducting airways (midlevel and RB); yet, this pattern did not coincide with preferential accumulation of specific immune cell populations in these regions. We did not perform an exhaustive analysis for all airway immune cells; it is possible that more specialized immune cell phenotypes preferentially accumulate within distal airways (i.e. unique T lymphocyte subsets, activated eosinophils). In asthmatic subjects, small airways exhibit a significant increase in activated eosinophils as compared with large airways; this finding is of particular importance as the degree of airways eosinophilia correlates with asthma severity [15, 17, 54]. Alternatively, structural cells within the distal airway microenvironment (i.e. epithelium, fibroblasts) could account for an additional source of cytokine/chemokine mRNA. *In situ* hybridization experiments

using distal airways of HDM monkeys supports the former postulate, in that detection of IL-4 mRNA was limited to cells of lymphoid origin.

It has been recently proposed that peripheral regions of the lung play a more significant role than proximal airways with regard to inflammatory events and airflow obstruction in allergic asthma [55]. From a structural standpoint, because the cumulative surface area and volume of the distal airways are much greater than proximal airways, inflammatory events associated with allergen challenge are much more pronounced in the peripheral lung. Further, the peripheral lung is a major site of airflow resistance in patients with asthma [56-59]. With findings from human subjects, our results suggest that the distal conducting airway is a specialized microenvironment for the acute pulmonary response to allergen challenge. It is well established that increased inflammation within the airways following allergen challenge is at least partially because of increased trafficking of immune cells from the vasculature; increased vascular expressions of ICAM-1, VCAM-1, and E-selectin in asthmatic subjects following allergen challenge provide important evidence of increased recruitment of immune cells in the acute pulmonary response [60-62]. In conjunction with adhesion molecules, both cytokines and chemokines contribute to the multi-step paradigm of leucocyte trafficking, either directly via chemotaxis or indirectly by inducing the expression of chemoattractants. Although adhesion molecules were not evaluated in this study, the finding of elevated expression of cytokines and chemokines within distal regions of the lung suggests that this site may be most important for the rapid mobilization of effector immune cells into the airways following allergen exposure; this could explain why immune cell abundance was not significantly increased in distal airway generations. Proximal airways, in contrast, may serve as a reservoir for immune cells that contribute to the chronic inflammatory response and remodeling with persistent allergen exposure. In conjunction with our previously reported findings for the animals evaluated in this study, the data suggest that elevated expression of key cytokines and increased volume of IgE^+ and $CD25^+$ cells in mid-level airways is associated with enhanced responsiveness to histamine challenge.

In summary, we have found that immune cells and cytokine/chemokine mediators that play an important role in the pathogenesis of allergic asthma are differentially distributed throughout the conducting airway tree. The patterns of immune cell distribution observed here in this study, both by airway generation and compartment within the airway wall, reflect the complex spatial organization of cellular mediators that direct multi-step trafficking of leucocytes from the vasculature into the lung. The precise pathophysiological role of the distal conducting airways in allergic asthma remains unclear. Our findings suggest that peripheral airways may be an important site for the acute pulmonary immune response to allergen challenge, and could be an excellent region to target for the development of therapeutic anti-inflammatory approaches in the future.

Acknowledgments

The authors of this paper would like to acknowledge the expert technical assistance of Brian Tarkington, Vivianna Wong, Jodie Usachenko, Joan Gerriets, and Sarah Davis during the course of this study. This study was supported by NIEHS ES-00628 (C. Plopper), NCRR RR00169, Tobacco Related Disease Research Program 6KT-0411 (L. Miller) and Tobacco Related Disease Research Program 8IT-0054 (L. Miller).

References

1. Busse WW, Lemanske RF. Asthma. N Engl J Med. 2001; 344:350–62. [PubMed: 11172168]
2. Tunon-De-Lara JM, Redington AE, Bradding P, et al. Dendritic cells in normal and asthmatic airways: expression of the alpha subunit of the high affinity immunoglobulin E receptor (Fc epsilon RI-alpha). Clin Exp Allergy. 1996; 26:648–55. [PubMed: 8809422]

3. Moller GM, Overbeek SE, van Helden-Meeuwsen CG, et al. Increased numbers of dendritic cells in the bronchial mucosa of atopic asthmatic patients: downregulation of inhaled corticosteroids. Clin Exp Allergy. 1996; 26:517–24. [PubMed: 8735863]

4. Bertorelli G, Bocchino V, Zhou X, et al. Dendritic cell number is related to IL-4 expression in the airways of atopic asthmatic subjects. Allergy. 2000; 55:449–54. [PubMed: 10843425]

5. Azzawi M, Bradley B, Jeffery PK, et al. Identification of activated T-lymphocytes and eosinophils in bronchial biopsies in stable atopic asthma. Am Rev Respir Dis. 1990; 142:1407–13. [PubMed: 2252260]

6. Bradley BL, Azzawi M, Jacobson M, et al. Eosinophils, T-lymphocytes, mast cells, neutrophils, and macrophages in bronchial biopsy specimens from atopic subjects with asthma: comparison with biopsy specimens from atopic subjects without asthma and normal control subjects and relationship to bronchial hyperresponsiveness. J Allergy Clin Immunol. 1991; 88:661–74. [PubMed: 1918731]

7. Bentley AM, Meng Q, Robinson DS, Hamid Q, Kay AB, Durham SR. Increases in activated T lymphocytes, eosinophils, and cytokine mRNA expression for interleukin-5 and granulocyte/macrophage colony-stimulating factor in bronchial biopsies after allergen inhalation challenge in atopic asthmatics. Am J Respir Cell Mol Biol. 1993; 8:35–42. [PubMed: 8417755]

8. Bellini A, Vittori E, Marini M, Ackerman V, Mattoli S. Intraepithelial dendritic cells and selective activation of Th2-like lymphocytes in patients with atopic asthma. Chest. 1993; 103:997–1005. [PubMed: 8131514]

9. Durham SR, Gould HJ, Thienes CP, et al. Expression of epsilon germ-line gene transcripts and mRNA for the epsilon heavy chain of IgE in nasal B cells and the effects of topical corticosteroid. Eur J Immunol. 1997; 27:2899–906. [PubMed: 9394816]

10. Wilson DR, Merrett TG, Varga EM, et al. Increases in allergenspecific IgE in BAL after segmental allergen challenge in atopic asthmatics. Am J Respir Crit Care Med. 2002; 165:22–6. [PubMed: 11779725]

11. Chung KF, Barnes PJ. Cytokines in asthma. Thorax. 1999; 54:825–57. [PubMed: 10456976]

12. Panina-Bordignon P, Papi A, Mariani M, et al. The C–C chemokine receptors CCR4 and CCR8 identify airway T cells of allergenchallenged atopic asthmatics. J Clin Invest. 2001; 107:1357–64. [PubMed: 11390417]

13. Ying S, Meng Q, Zeibecoglou K, et al. Eosinophil chemotactic chemokines (eotaxin, eotaxin-2, RANTES, monocyte chemoattractant protein-3 (MCP-3), and MCP-4), and C-C chemokine receptor 3 expression in bronchial biopsies from atopic and nonatopic (Intrinsic) asthmatics. J Immunol. 1999; 163:6321–9. [PubMed: 10570327]

14. Haley KJ, Sunday ME, Wiggs BR, et al. Inflammatory cell distribution within and along asthmatic airways. Am J Respri Crit Care Med. 1998; 158:565–72.

15. Carroll N, Cooke C, James A. The distribution of eosinophils and lymphocytes in the large and small airways of asthmatics. Eur Respir J. 1997; 10:292–300. [PubMed: 9042623]

16. Hamid Q. Gross pathology and histopathology of asthma. J Allergy Clin Immunol. 2003; 111:431–2. [PubMed: 12589370]

17. Hamid Q, Song Y, Kotsimbos TC, et al. Inflammation of small airways in asthma. J Allergy Clin Immunol. 1997; 100:44–51. [PubMed: 9257786]

18. Minshall EM, Hogg JC, Hamid QA. Cytokine mRNA expression in asthma is not restricted to the large airways. J Allergy Clin Immunol. 1998; 101:386–90. [PubMed: 9525456]

19. Schelegle ES, Gershwin LJ, Miller LA, et al. Allergic asthma induced in rhesus monkeys by house dust mite (dermatophadoides farinae). Am J Pathol. 2001; 158:333–41. [PubMed: 11141508]

20. Hyde DM, Miller LA, McDonald RJ, et al. Neutrophils enhance clearance of necrotic epithelial cells in ozone-induced lung injury in rhesus monkeys. Am J Physiol. 1999; 277:L1190–8. [PubMed: 10600890]

21. Duan X, Buckpitt AR, Plopper CG. Variation in antioxidant enzyme activities in anatomic subcompartments within rat and rhesus monkey lung. Toxicol Appl Pharmacol. 1993; 123:73–82. [PubMed: 8236264]

22. Hurst SD, Muchamuel T, Gorman DM, et al. New IL-17 family members promote Th1 or Th2 responses in the lung: in vivo function of the novel cytokine IL-25. J Immunol. 2002; 169:443–53. [PubMed: 12077275]

23. Gundel RH, Kinkade P, Torcellini CA, et al. Antigen-induced mediator release in primates. Am Rev Respir Dis. 1991; 144:76–82. [PubMed: 1648317]
24. Miadonna A, Tedeschi A, Brasca C, Folco G, Sala A, Murphy RC. Mediator release after endobronchial antigen challenge in patients with respiratory allergy. J Allergy Clin Immunol. 1990; 85:906–13. [PubMed: 1692050]
25. Reimann KA, Waite BCD, Lee-Parritz DE, et al. Use of human leukocyte-specific monoclonal antibodies for clinically immunophenotyping lymphocytes of rhesus monkeys. Cytometry. 1994; 17:102–8. [PubMed: 8001455]
26. Wagner G. E-cadherin: a distant member of the immunoglobulin superfamily. Science. 1995; 267:342. [PubMed: 7824932]
27. Wells E, Harper ST, Jackson CG, Mann J, Eady RP. Characterization of primate bronchoalveolar mast cells. I. IgE-dependent release of histamine, leukotrienes, and prostaglandins. J Immunol. 1986; 137:3933–40.
28. Yasue M, Nakamura S, Yokota T, Okudaira H, Okumura Y. Experimental monkey model sensitized with mite antigen. Int Arch Allergy Immunol. 1998; 115:303–11. [PubMed: 9566353]
29. Plopper CG, Heidsiek JG, Weir AJ, George JA, Hyde DM. Tracheobronchial epithelium in the adult rhesus monkey: a quantitative histochemical and ultrastructural study. Am J Anat. 1989; 184:31–40. [PubMed: 2916437]
30. Plopper CG, Alley JL, Weir AJ. Differentiation of tracheal epithelium during fetal lung maturation in the rhesus monkey Macaca mulatta. Am J Anat. 1986; 175:59–71. [PubMed: 3953471]
31. Plopper CG, Weir AJ, Nishio SJ, Cranz DL, St George JA. Tracheal submucosal gland development in the rhesus monkey, Macaca mulatta: ultrastructure and histochemistry. Anat Embryol (Berl). 1986; 174:167–78. [PubMed: 3740452]
32. Plopper C, George JS, Cardoso W, Wu R, Pinkerton K, Buckpitt A. Development of airway epithelium: patterns of expression for markers of differentiation. Chest. 1992; 101:2S–5S. [PubMed: 1371732]
33. Shortman K, Liu YJ. Mouse and human dendritic cell subtypes. Nat Rev Immunol. 2002; 2:151–61. [PubMed: 11913066]
34. Ordonez C, Ferrando R, Hyde DM, Wong HH, Fahy JV. Epithelial desquamation in asthma: artifact or pathology? Am J Respir Crit Care Med. 2000; 162:2324–9. [PubMed: 11112158]
35. Demedts IK, Brusselle GG, Vermaelen KY, Pauwels RA. Identification and characterization of human pulmonary dendritic cells. Am J Resp Cell Mol Biol. 2005; 32:177–84.
36. Uchiyama T, Broder S, Waldmann TA. A monoclonal antibody (anti-Tac) reactive with activated and functionally mature T cells. I. Production of anti-Tac monoclonal antibody and distribution of Tac(1) cells. J Immunol. 1981; 126:1393–403.
37. Mittler R, Rao P, Olini G, et al. Activated human Be cells display a functional IL-2 receptor. J Immunol. 1985; 134:2393–9. [PubMed: 2982945]
38. Rand TH, Silberstein DS, Kornfeld H, Weller PF. Human eosinophils express functional interleukin 2 receptors. J Clin Invest. 1991; 88:825–32. [PubMed: 1885772]
39. Snow RE, Djukanovic R, Stevenson FK. Analysis of immunoglobulin E VH transcripts in a bronchial biopsy of an asthmatic patient confirms bias towards VH5, and indicates local clonal expansion, somatic mutation and isotype switch events. Immunology. 1999; 98:646–51. [PubMed: 10594700]
40. Crimi E, Scordamaglia A, Crimi P, Zupo S, Barocci S. Total and specific IgE in serum, bronchial lavage and bronchoalveolar lavage of asthmatic patients. Allergy. 1983; 38:553–9. [PubMed: 6660434]
41. Campbell AM, Vachier I, Chanez P, et al. Expression of the highaffinity receptor for IgE on bronchial epithelial cells of asthmatics. Am J Respir Cell Mol Biol. 1998; 19:92–7. [PubMed: 9651184]
42. Wardlaw AJ, Dunnette S, Gleich GJ, Collins JV, Kay AB. Eosinophils and mast cells in bronchoalveolar lavage in subjects with mild asthma. Relationship to bronchial hyperreactivity. Am Rev Respir Dis. 1988; 137:62–9.
43. De Monchy JG, Kauffman HF, Venge P, et al. Bronchoalveolar eosinophilia during allergen-induced late asthmatic reactions. Am Rev Respir Dis. 1985; 131:373–6. [PubMed: 3977174]

44. Hamid Q, Azzawi M, Ying S, et al. Expression of mRNA for interleukin-5 in mucosal bronchial biopsies from asthma. J Clin Invest. 1991; 87:1541–6. [PubMed: 2022726]
45. Robinson DS, Ying S, Bentley AM, et al. Relationships among numbers of bronchoalveolar lavage cells expressing messenger ribonucleic acid for cytokines, asthma symptoms, and airway methacholine responsiveness in atopic asthma. J Allergy Clin Immunol. 1993; 92:397–403. [PubMed: 8360390]
46. Humbert M, Durham SR, Ying S, et al. IL-4 and IL-5 mRNA and protein in bronchial biopsies from patients with atopic and nonatopic asthma: evidence against “intrinsic” asthma being a distinct immunopathologic entity. Am J Respir Crit Care Med. 1996; 154:1497–504. [PubMed: 8912771]
47. Humbert M, Corrigan CJ, Kimmitt P, Till SJ, Kay AB, Durham SR. Relationship between IL-4 and IL-5 mRNA expression and disease severity in atopic asthma. Am J Respir Crit Care Med. 1997; 156:704–8. [PubMed: 9309982]
48. Humbert M, Durham SR, Kimmitt P, et al. Elevated expression of messenger ribonucleic acid encoding IL-13 in the bronchial mucosa of atopic and nonatopic subjects with asthma. J Allergy Clin Immunol. 1997; 99:657–65. [PubMed: 9155833]
49. Walter MJ, Kajiwara N, Karanja P, Castro M, Holtzman MJ. Interleukin 12 p40 production by barrier epithelial cells during airway inflammation. J Exp Med. 2001; 193:339–51. [PubMed: 11157054]
50. Campbell JJ, Bowman EP, Murphy K, et al. 6-C-kine (SLC), a lymphocyte adhesion-triggering chemokine expressed by high endothelium, is an agonist for the MIP-3beta receptor CCR7. J Cell Biol. 1998; 141:1053–9. [PubMed: 9585422]
51. Sallusto F, Schaerli P, Loetscher P, et al. Rapid and coordinated switch in chemokine receptor expression during dendritic cell maturation. Eur J Immunol. 1998; 28:2760–9. [PubMed: 9754563]
52. Julia V, Hessel EM, Malherbe L, Glaichenhaus N, O’Garra A, Coffman RL. A restricted subset of dendritic cells captures airborne antigens and remains able to activate specific T cells long after antigen exposure. Immunity. 2002; 16:271–83. [PubMed: 11869687]
53. Salvi S, Babu K, Holgate S. Is asthma really due to a polarized T cell response toward a helper T cell type 2 phenotype? Am J Respir Crit Care Med. 2001; 164:1343–6. [PubMed: 11704578]
54. Synek M, Beasley R, Frew AJ, et al. Cellular infiltration of the airways in asthma of varying severity. Am J Respir Crit Care Med. 1996; 154:224–30. [PubMed: 8680684]
55. Tulic MK, Christodoulopoulos P, Hamid Q. Small airway inflammation in asthma. Respir Res. 2001; 2:333–9. [PubMed: 11737932]
56. Wagner EM, Liu MC, Weinmann GG, Permutt S, Bleecker ER. Peripheral lung resistance in normal and asthmatic subjects. Am Rev Respir Dis. 1990; 141:584–8. [PubMed: 2178524]
57. Ingram RH Jr. Physiological assessment of inflammation in the peripheral lung of asthmatic patients. Lung. 1990; 168:237–47. [PubMed: 2126831]
58. Yanai M, Sekizawa K, Ohrui T, Sasaki H, Takishima T. Site of airway obstruction in pulmonary disease: direct measurement of intrabronchial pressure. J Appl Physiol. 1992; 72:1016–23. [PubMed: 1568955]
59. Wagner EM, Bleecker ER, Permutt S, Liu MC. Direct assessment of small airways reactivity in human subjects. Am J Respir Crit Care Med. 1998; 157:447–52. [PubMed: 9476856]
60. Gosset P, Tillie-Leblond I, Janin A, et al. Expression of E-selectin, ICAM-1 and VCAM-1 on bronchial biopsies from allergic and non-allergic asthmatic patients. Int Arch Allergy Immunol. 1995; 106:69–77. [PubMed: 7529075]
61. Ohkawara Y, Yamauchi K, Maruyama N, et al. In situ expression of the cell adhesion molecules in bronchial tissues from asthmatics with air flow limitation: in vivo evidence of VCAM-1/VLA-4 interaction in selective eosinophil infiltration. Am J Respir Cell Mol Biol. 1995; 12:4–12. [PubMed: 7529029]
62. Bentley AM, Durham SR, Robinson DS, et al. Expression of endothelial and leukocyte adhesion molecules interacellular adhesion molecule-1, E-selectin, and vascular cell adhesion molecule-1 in the bronchial mucosa in steady-state and allergen-induced asthma. J Allergy Clin Immunol. 1993; 92:857–68. [PubMed: 7505008]

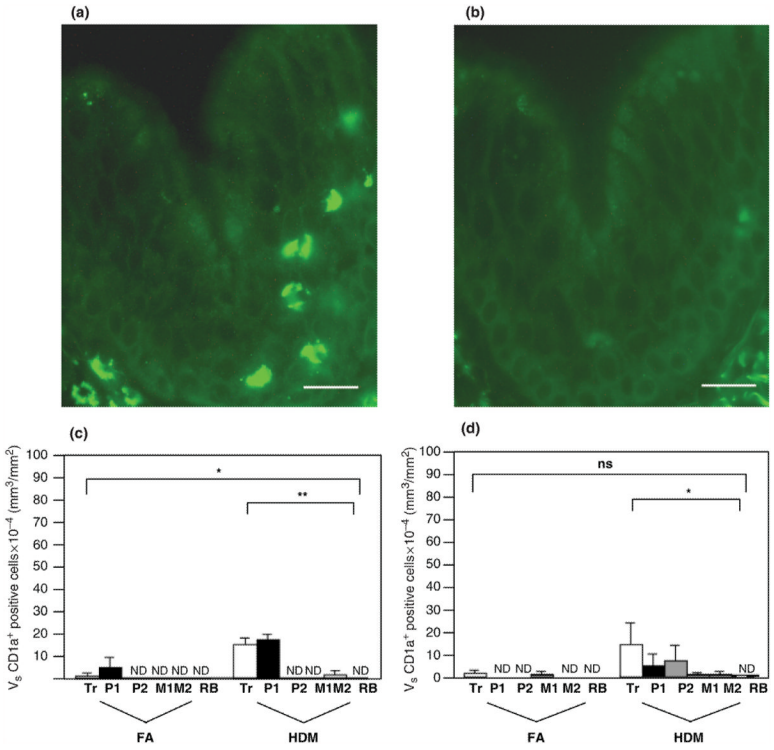

Fig. 1.

Distribution of CD1a$^+$ dendritic cells within airway mucosa of HDM-challenged rhesus monkeys. CD1a$^+$ dendritic cells were identified by immunofluorescence staining of trachea and left caudal lobe sections obtained from HDM-challenged monkeys. Tr, P1, P2, M1, M2, and RB represent cryosections obtained from tissue blocks of trachea and regions progressively representing the most proximal (P1) to distal (RB) intrapulmonary airways of the lobe. Columns represent the average volume ± SE of CD1a$^+$ staining cells (mm^3) with respect to the surface area of basal lamina (mm^2). FA, filtered air control; HDM, house dust mite-challenged; RB, respiratory bronchiole. (a) CD1a$^+$ immunofluorescence staining of trachea from a representative HDM monkey. Bar=20 μm. (b) Control staining of an adjacent section using an FITC-conjugated o mouse IgG1 isotype control. Bar=20 μm. (c) Abundance of CD1a$^+$ cells within the epithelial compartment of conducting airways. ND, none detected; *P<0.0001 by analysis of variance (block effect); **P=0.0005 by analysis of variance (treatment effect). (d) Abundance of CD1a$^+$ cells within the interstitial compartment of conducting airways. *P=0.0284 by analysis of variance (treatment effect).

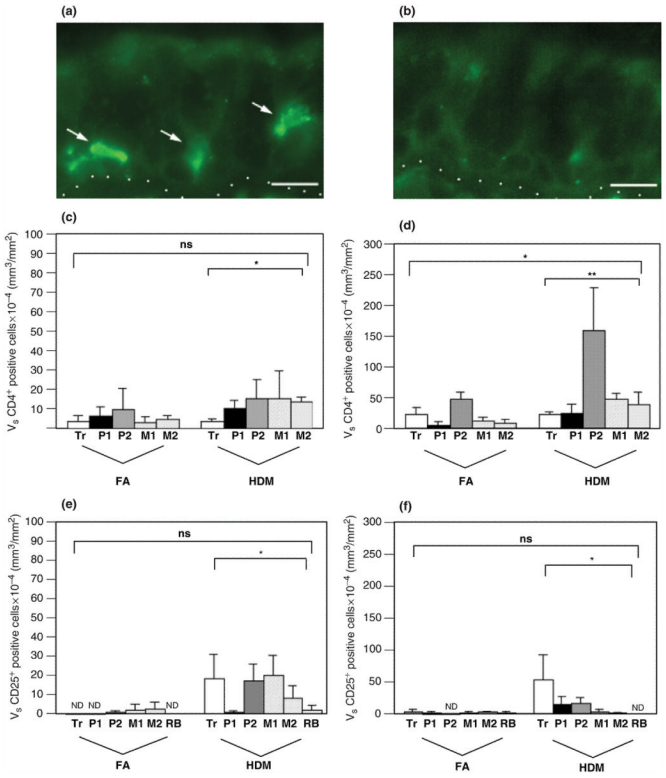

Fig. 2.

Distribution of $CD4^+$ lymphocytes and $CD25^+$ cells within airway mucosa of HDM-challenged rhesus monkeys. $CD3^+/CD4^+$ lymphocytes and $CD25^+$ cells were quantitated by immunofluorescence staining of trachea and left caudal lobe sections obtained from HDM-challenged monkeys. Tr, P1, P2, M1, M2, and RB represent cryosections obtained from tissue blocks of trachea and regions progressively representing the most proximal (P1) to distal (RB) intrapulmonary airways of the lobe. Columns represent the average volume ± SE of $CD3^+/CD4^+$ or $CD25^+$ staining cells (mm^3) with respect to the surface area of basal lamina (mm^2). FA, filtered air control; HDM, house dust mite-challenged; RB, respiratory bronchiole. (a) $CD25^+$ immunofluorescence staining of a mid-level intrapulmonary airway (M1) from a representative HDM monkey. The dotted line defines the basement membrane of the region; the epithelium is above the line, and the interstitium is below the line. Arrows point to three $CD25^+$ cells (green) within the epithelium. Bar=10 μm. (b) Control staining of an adjacent section using an FITC-conjugated mouse IgG_1 isotype control. Bar=10 μm. (c) Abundance of $CD3^+/CD4^+$ fluorescence double-positive lymphocytes within the epithelial compartment of conducting airways. **P*=0.07 by analysis of variance (treatment effect). (d) Abundance of $CD3^+/CD4^+$ fluorescence double-positive lymphocytes within the interstitial compartment of conducting airways. **P*=0.0007 by analysis of variance (block effect); ***P*=0.0037 by analysis of variance (treatment effect). (e) Abundance of $CD25^+$ cells within the epithelial compartment of conducting airways. **P*=0.0044 by analysis of variance (treatment effect). (f) Abundance of $CD25^+$ cells within the interstitial compartment of conducting airways. **P*=0.0818 by analysis of variance (treatment effect).

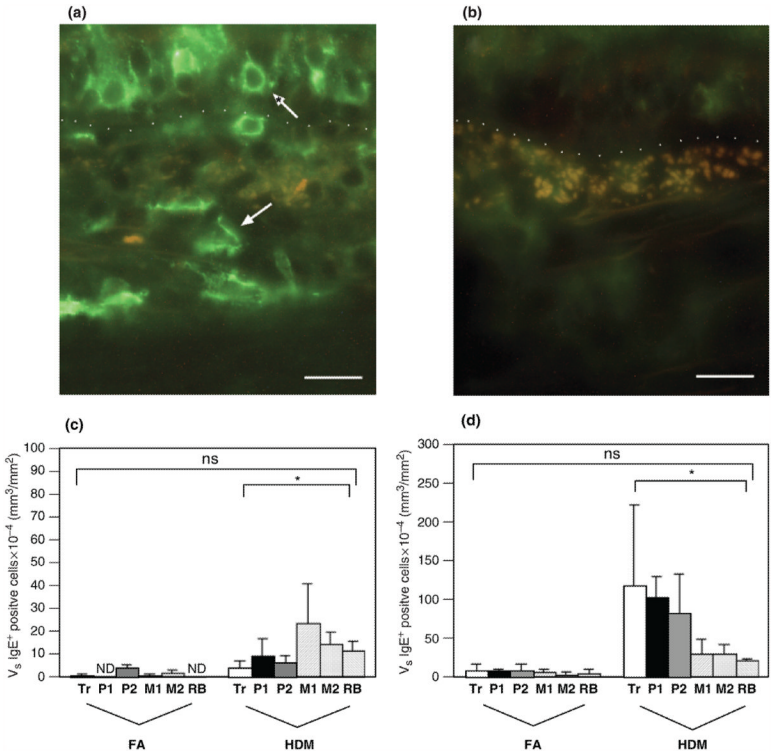

Fig. 3.

Distribution of IgE$^+$ cells within airway mucosa of HDM-challenged rhesus monkeys. IgE$^+$ cells were quantitated by immunofluorescence staining of trachea and left caudal lobe sections obtained from HDM-challenged monkeys. Tr, P1, P2, M1, M2, and RB represent cryosections obtained from tissue blocks of trachea and regions progressively representing the most proximal (P1) to distal (RB) intrapulmonary airways of the lobe. Columns represent the average volume ± SE of IgE$^+$ staining cells (mm^3) within the specified compartment with respect to the surface area of basal lamina (mm^2). FA, filtered air control; HDM, house dust mite-challenged; RB, respiratory bronchiole. (a) IgE$^+$ immunofluorescence staining of an intrapulmonary airway (block P2) from a representative HDM-challenged monkey. The dotted line defines the basement membrane; the epithelium is above the line, and the interstitium is below the line. The normal arrow points to an interstitial IgE$^+$ cell; the *arrow points to an epithelial IgE$^+$ cell. Bar=20 μm. (b) Control staining of an adjacent section using non-specific goat IgG and ALEXA 488 secondary antibody. Bar=20 μm. (c) Abundance of IgE$^+$ cells within the epithelial compartment of conducting airways. *P=0.0088 by analysis of variance (treatment effect). (d) Abundance of IgE$^+$ cells within the interstitial compartment of conducting airways. *P=0.0125 by analysis of variance (treatment effect).

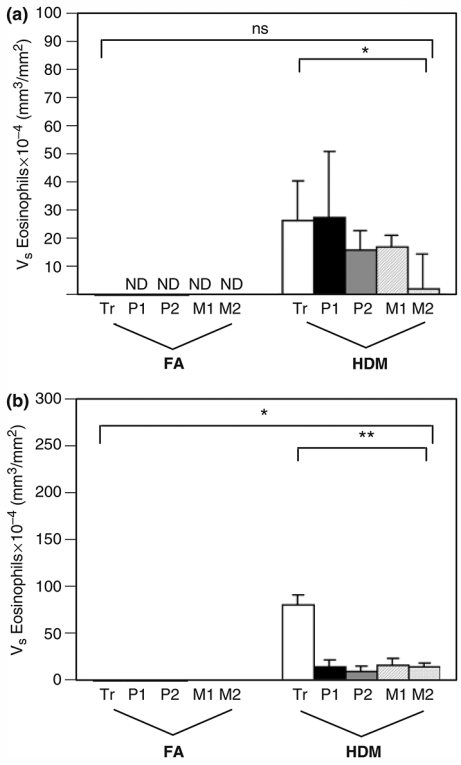

Fig. 4.

Distribution of eosinophils within airway mucosa of HDM-challenged rhesus monkeys. Eosinophils were quantitated from H&E staining of trachea and right middle lobe sections obtained from HDM-challenged monkeys. Tr, P1, P2, M1, and M2 represent cryosections obtained from tissue blocks of trachea and regions progressively representing the most proximal (P1) to mid-level intrapulmonary airways of the lobe. Columns represent the average volume ± SE of eosinophils (mm^3) within the specified compartment with respect to the surface area of basal lamina (mm^2). FA, filtered air control; HDM, house dust mite-challenged. (a) Abundance of eosinophils within the epithelial compartment of conducting airways. **P*=0.0046 by analysis of variance (treatment effect). (b) Abundance of eosinophils within the interstitial compartment of conducting airways. **P*<0.0001 by analysis of variance (block effect); ***P*<0.0001 by analysis of variance (treatment effect).

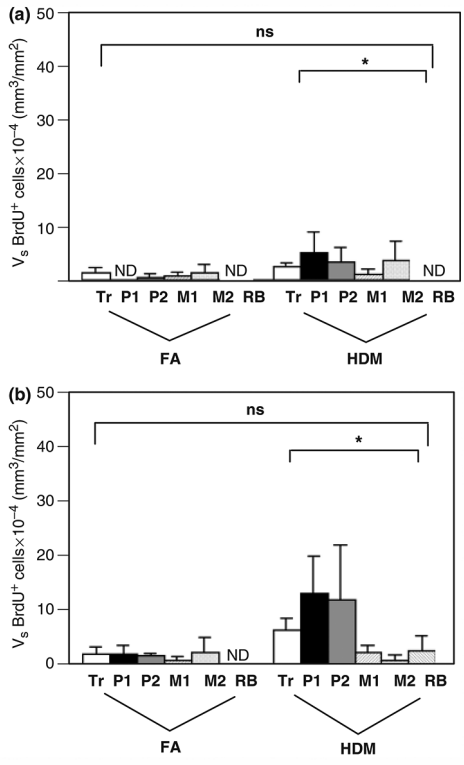

Fig. 5.

Distribution of proliferating cells within airway mucosa of HDM-challenged rhesus monkeys. Proliferating cells were quantitated by immunostaining for 5-bromo-2′deoxyuridine (BrdU) incorporation in the trachea and left caudal lobe sections obtained from HDM-challenged monkeys. Tr, P1, P2, M1, M2, and RB represent cryosections obtained from tissue blocks of the trachea and regions progressively representing the most proximal (P1) to distal (RB) intrapulmonary airways of the lobe. Columns represent the average volume ± SE of $BrdU^+$ cells (mm^3) within the specified compartment with respect to the surface area of basal lamina (mm^2). FA, filtered air control; HDM, house dust mite-challenged; RB, respiratory bronchiole. (a) Abundance of $BrdU^+$ cells within the epithelial compartment of conducting airways. **P*=0.0708 by analysis of variance (treatment effect). (b) Abundance of $BrdU^+$ cells within the interstitial compartment of conducting airways. **P*=0.0410 by analysis of variance (treatment effect).

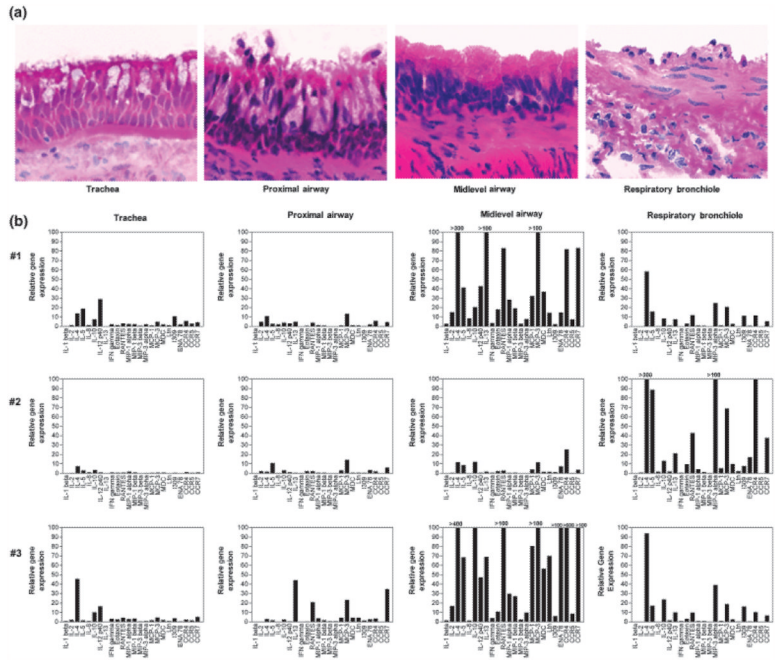

Fig. 6.

Cytokine and chemokine gene expression within airway mucosa of house dust mite (HDM)-challenged rhesus monkeys. The relative mRNA expression of the listed cytokines, chemokines, and chemokine receptors were evaluated from trachea and microdissected intrapulmonary airways obtained from the right caudal lobe of HDM-challenged monkeys. Samples were collected from the trachea, most proximal intrapulmonary airway, a midlevel airway, and RB for RNA isolation; separately collected samples from each airway generation were processed for histology. (a) H&E staining of microdissected samples, showing both epithelial and interstitial organization of each airway generation. (b) Relative mRNA expression profile for different airway generations in three (#1, #2, #3) different HDM-challenged monkeys. Relative gene expression for each cytokine, chemokine, or chemokine receptor was determined from averaged Ct values from a pool of five control monkeys.

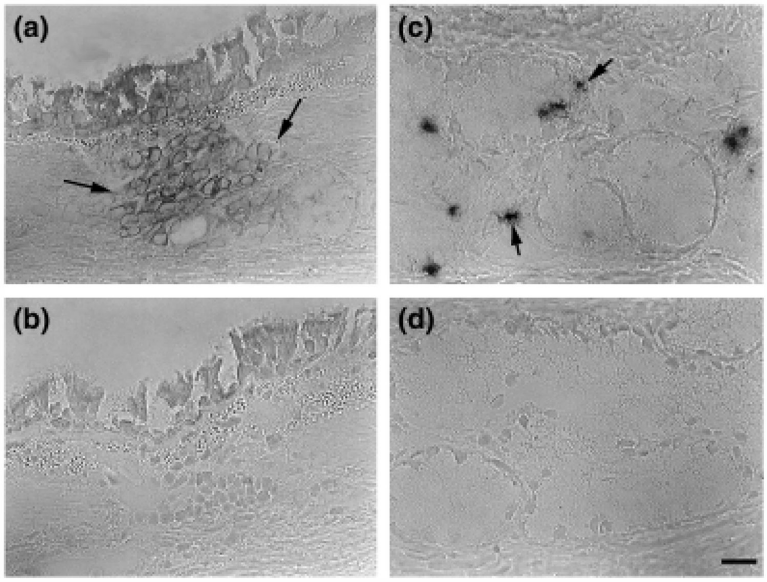

Fig. 7.

Cellular distribution of IL-4 gene expression within airway mucosa of house dust mite (HDM)-challenged rhesus monkeys. Localization of IL-4 mRNA within airway mucosa was determined by *in situ* hybridization using cryosections from a representative HDM-challenged animal (animal #1 in Fig. 6). (a, c) Sections labelled with anti-sense strand IL-4 RNA probe. Arrows point to positive cells within the subepithelial region (a) as well as glands (c). (b, d) Control sections for (a) and (c) labelled with sense strand IL-4 RNA probe. Bar=20 μm.